

Published in final edited form as:

*Eur J Neurosci*. 2009 July ; 30(1): 57–64. doi:10.1111/j.1460-9568.2009.06789.x.

## Deletion of TASK1 and TASK3 channels disrupts intrinsic excitability but does not abolish glucose or pH responses of orexin/hypocretin neurons

J. A. González<sup>1</sup>, Lise T. Jensen<sup>2</sup>, Susan E. Doyle<sup>3</sup>, Manuel Miranda-Anaya<sup>4</sup>, Michael Menaker<sup>3</sup>, Lars Fugger<sup>5</sup>, Douglas A. Bayliss<sup>6</sup>, and Denis Burdakov<sup>1</sup>

<sup>1</sup>Department of Pharmacology, University of Cambridge, Cambridge CB2 1 PD, UK

<sup>2</sup>Clinical Institute, Aarhus University Hospital, Skejby Sygehus, Denmark

<sup>3</sup>Department of Biology, University of Virginia, Charlottesville, Virginia, USA

<sup>4</sup>Departamento de Biología Celular, Facultad de Ciencias, Universidad Nacional Autónoma de México, México City, México

<sup>5</sup>Department of Clinical Neurology, Weatherall Institute of Molecular Medicine, University of Oxford, Oxford, UK

<sup>6</sup>Department of Pharmacology, University of Virginia, Charlottesville, Virginia, USA

### Abstract

The firing of hypothalamic hypocretin/orexin neurons is vital for normal sleep–wake transitions, but its molecular determinants are not well understood. It was recently proposed that TASK (TWIK-related acid-sensitive potassium) channels [TASK1 (K<sub>2p</sub>3.1) and/or TASK3 (K<sub>2p</sub>9.1)] regulate neuronal firing and may contribute to the specialized responses of orexin neurons to glucose and pH. Here we tested these theories by performing patch-clamp recordings from orexin neurons directly identified by targeted green fluorescent protein labelling in brain slices from TASK1/3 double-knockout mice. The deletion of TASK1/3 channels significantly reduced the ability of orexin cells to generate high-frequency firing. Consistent with reduced excitability, individual action potentials from knockout cells had lower rates of rise, higher thresholds and more depolarized after-hyperpolarizations. However, orexin neurons from TASK1/3 knockout mice retained typical responses to glucose and pH, and the knockout animals showed normal food-anticipatory locomotor activity. Our results support a novel role for TASK genes in enhancing neuronal excitability and promoting high-frequency firing, but suggest that TASK1/3 subunits are not essential for orexin cell responses to glucose and pH.

### Keywords

appetite; firing; glucose; hypothalamus; K channels; mice; sleep

### Introduction

In mammals, appropriate matching of behaviour and brain state to the environment critically relies on neurons containing peptide transmitters hypocretins/orexins (de Lecea *et al.*, 1998;

Sakurai *et al.*, 1998; Sakurai, 2007). These cells (hereafter called orexin neurons) are located in the lateral hypothalamus but innervate most of the brain, where orexins cause neuronal excitation by acting on specific G-protein-coupled receptors (Peyron *et al.*, 1998; Sakurai, 2007). The firing of orexin neurons stimulates awakening (Adamantidis *et al.*, 2007), and is so critical for sustained arousal that loss of orexin cells causes severe narcolepsy/cataplexy (Hara *et al.*, 2001). In addition, orexin neurons play key roles in reward-seeking and stress-induced drug relapse (Winsky-Sommerer *et al.*, 2004; Boutrel *et al.*, 2005; Harris *et al.*, 2005).

Despite the importance of orexin neurons for behavioural coordination, much remains unknown about the molecular mechanisms controlling their firing. Orexin cells generate spontaneous Na<sup>+</sup>-dependent action potentials *in vitro* (Li *et al.*, 2002; Eggermann *et al.*, 2003), but little is known about the molecular identity of ion channels that determine the shape of these action potentials. In turn, several ion channels have been proposed to underlie stimulus-induced control of orexin cell firing (e.g. Burdakov *et al.*, 2006; Li & van den Pol, 2008; Tsunematsu *et al.*, 2008), but their identities have not been explored by manipulation of candidate channel genes.

'Two-pore-domain' K<sup>+</sup> (K<sub>2p</sub>) channels, encoded by the KCNK gene family, are the largest but functionally least understood group of K<sup>+</sup> channels (Lesage & Lazdunski, 2000; Goldstein *et al.*, 2001; Patel & Honore, 2001). Recently, two members of this family, TASK1 (K<sub>2p3.1</sub>) and TASK3 (K<sub>2p9.1</sub>), which form 'leak' channels inhibited by low pH, have been proposed to play key roles in the control of neuronal firing. Based on data from cerebellar granule neurons, Brickley *et al.* (2007) proposed that TASK3-containing channels have a novel effect of increasing membrane excitability. Based on biophysical and pharmacological data from orexin neurons, we hypothesized that in these cells, TASK (TWIK-related acid-sensitive potassium)-like channels may contribute to K<sup>+</sup> currents triggered by elevations in extracellular glucose levels and by falls in extracellular proton concentration (Burdakov *et al.*, 2006; Williams *et al.*, 2007).

In the present study, we examine these theories in identified orexin neurons by creating transgenic mice that lack TASK1/3 channels and express green fluorescent protein (GFP) under the control of the *pre-proorexin* promoter.

## Methods

### Generation of transgenic mice

To rule out probable compensation between TASK1 and TASK3 channels, we used TASK1/3 double knockout mice, which were generated and validated as previously described (Mulkey *et al.*, 2007). To create TASK1/3 knockout mice with GFP-labelled orexin neurons, we crossed the knockout mice with orexin-eGFP mice, generated and validated as described in (Burdakov *et al.*, 2006). F1 breeder mice expressing eGFP were identified by PCR amplification of tail tip DNA using primers specific for the orexin-eGFP construct and backcrossed to TASK1/3 knockout mice. F2 mice expressing eGFP were tested for the TASK1 and TASK3 knockout mutations by multiplex PCRs using primers across loxP sites and spanning the deleted regions as previously described (Mulkey *et al.*, 2007). Finally, eGFP-expressing mice with homozygotic disruption of the TASK1 and TASK3 genes were intercrossed, and genotyped offspring were used for experiments.

### Electrophysiology

Preparation of acute brain slices and subsequent whole-cell patch-clamp recordings were performed as described in Burdakov *et al.* (2006). Animals were killed by cervical dislocation. All procedures were in accordance with the Animals (Scientific Procedures) Act

1986 (United Kingdom). All recordings were performed at 36°C. In all experiments except those detailed in Figs 4A–C and 5, extracellular solution was standard artificial cerebrospinal fluid (ACSF), containing (in mM): NaCl 125, KCl 2.5, MgCl<sub>2</sub> 2, NaH<sub>2</sub>PO<sub>4</sub> 1.2, NaHCO<sub>3</sub> 21, CaCl<sub>2</sub> 2 and glucose 1, bubbled with 95% O<sub>2</sub> and 5% CO<sub>2</sub>. In the experiments detailed in Figs 4A–C and 5, we used a HEPES-buffered ACSF to attain greater pH control (Williams *et al.*, 2007), which contained (in mM): NaCl 118, KCl 3, MgCl<sub>2</sub> 1, CaCl<sub>2</sub> 1.5, HEPES 25 and glucose 1, pH adjusted with NaOH, and bubbled with 100% O<sub>2</sub>. Voltage-clamp recordings (and current-clamp recordings in Fig. 5A, B) were performed using a potassium chloride pipette solution (in mM): KCl 130, HEPES 10, EGTA 1, MgCl<sub>2</sub> 2, K<sub>2</sub>ATP 5 and NaCl 2. Current-clamp recordings were performed using a potassium gluconate pipette solution (in mM): K-gluconate 120, HEPES 10, KCl 10, EGTA 1, MgCl<sub>2</sub> 2, K<sub>2</sub>ATP 4 and Na<sub>2</sub>ATP 1. Experiments detailed in Figs 1–3 were performed in the presence of blockers of synaptic communication (added to ACSF: D-AP5 50 μM, CNQX 10 μM, picrotoxin 50 μM). To create similar conditions for all cells during the analysis of action potential firing, in Fig. 2 all cells were held at –60 mV before the current injection (see Fig. 2A), while in Fig. 3 the action potentials were recorded from the same baseline potential (–30 mV), adjusted by sustained current injection. An EPC-10 patch-clamp amplifier operated using PATCHMASTER software (both from HEKA, Freiburg, Germany) was used for data acquisition. All the chemicals were from Sigma (St Louis, MO, USA), except for CNQX and D-AP5, which were from Tocris (Ellisville, MO, USA).

### Data analysis

Resting membrane potentials were taken as zero-current potentials in whole-cell current–voltage relationships obtained using the voltage-clamp ramps shown in Fig. 1 (in spontaneously spiking neurons, this method is more accurate than current-clamp). Input resistance was measured as the inverse of the slope (linear fit) of the current–voltage relationship between –80 and –60 mV. Firing–current relationships (Fig. 2B, C) were obtained from firing caused by slow ramp-like excitatory current injections (Fig. 2A), by plotting the inverse of each inter-spike interval (in seconds, *y*-axis) against the corresponding current (*x*-axis). For statistical analysis, these data were normalized to cell size, by dividing the current applied by the membrane capacitance, and then binned into 1-pA/pF bins (Fig. 2C).

Standard phase-plane analysis (plot of rate of change of membrane potential at each value of the membrane potential, Fig. 3C) was performed as described in Bean (2007). To calculate action potential thresholds, we used the ‘3rd derivative’ method described in Henze & Buzsáki (2001) and shown diagrammatically in Fig. 3D.

In Figs 4C and 5E, the net current–voltage relationship was fitted with the Goldman–Hodgkin–Katz (GHK) current equation in the following form

$$I = P_K z^2 \frac{VF^2}{RT} \frac{[K^+]_i - [K^+]_o \exp(-zFV/RT)}{1 - \exp(-zFV/RT)}$$

Here, *I* is current (in A), *V* is membrane potential (in V), *z* is the charge of a potassium ion (+1),  $[K^+]_i$  is the pipette K<sup>+</sup> concentration (in mM),  $[K^+]_o$  is the ACSF K<sup>+</sup> concentration (in mM), *T* is temperature (Kelvin), and *R* and *F* are standard parameters (Hille, 2001). *P<sub>K</sub>* (a constant reflecting the K<sup>+</sup> permeability of the membrane) was the only free parameter during fits. The value of *P<sub>K</sub>* used to obtain the fit shown in Fig. 4C was  $3.22 \times 10^{-17}$  cm/s, and that for Fig. 5E was  $8.73 \times 10^{-18}$  cm/s. Values are presented as means ± SEM. Statistical significance was evaluated using Student’s *t*-test for two independent samples, unless stated otherwise.

## Locomotor activity recordings and food restriction paradigm

Behavioural experiments were approved by the University of Virginia Animal Care and Use Committee and were in compliance with the Association for Assessment of Laboratory Animal Care guidelines. Male and female mice (~9 months of age) were housed in individual running wheel cages inside light-tight boxes under a 12/12-h light–dark cycle (lights on at 05: 00 and off at 17: 00 h). Temperature and humidity inside the boxes were maintained at 21°C and 50%, respectively. Wheel revolutions were recorded in 1-min bins, and analysed with CLOCKLAB software (Actimetrics, Wilmette, IL, USA). Water was available *ad libitum* throughout the experiment.

Animals were introduced to a 4-h food restriction paradigm as follows. A dish containing 5 g of powdered rodent breeder chow (Harlan-Techlad, 8664) mixed with water and 20% peanut butter was placed on the floor of each animal's cage at 08: 00 h and removed 10 hours later at 18: 00. Over the next 6 days, the time of food availability was decreased by removing food at progressively earlier times until food was available for 4 h only, from 08: 00 to 12: 00 h. After 3 days of 4-h food restriction, peanut butter was removed from the food mix and the 4-h restriction paradigm was continued for 15 more days. Animals were fasted for 2 days at the end of the experiment.

## Results

### Passive membrane properties of orexin neurons

Comparison of membrane current–voltage relationships of knockout and wild-type orexin neurons (hereafter KO and WT cells, respectively) showed a reduction in current with a reversal potential close to that of  $K^+$  (Fig. 1B). The outward current at  $-20$  mV was significantly reduced in KO cells relative to WT cells ( $263 \pm 23$  and  $452 \pm 87$  pA, respectively,  $t_{20} = 2.96$ ,  $P = 0.008$ ). KO cells had slightly more positive resting membrane potentials than WT cells ( $-60.6 \pm 2.1$  and  $-68 \pm 3.9$  mV, respectively,  $t_{20} = 1.78$ ,  $P = 0.09$ ,  $n > 5$  for each group), while their input resistance tended to be higher (KO,  $504 \pm 70$  M $\Omega$ ; WT,  $264 \pm 59$  M $\Omega$ ;  $t_{20} = 2$ ,  $P = 0.06$ ,  $n > 5$ ). These alterations are consistent with removal of a leak  $K^+$  channel from the orexin cell membrane, and suggest that postsynaptic TASK channels may contribute to the electrical properties of orexin neurons.

### Active membrane properties of orexin neurons

Spontaneous firing rates tended to be slightly higher in WT cells ( $13.8 \pm 2.1$  Hz) than in KO cells ( $9.4 \pm 2.6$  Hz), but this did not reach significance ( $P = 0.21$ ,  $n = 7$  for each group). The relationships between firing rate and stimulus current in KO and WT cells were similar at low stimulus levels, but diverged significantly at higher stimulus intensities, where KO cells were unable to reach the high firing rates seen in WT cells (Fig. 2). Phase-plane analysis of action potentials initiated from the same baseline potential (Fig. 3A–C) revealed significantly lower rates of action potential rise in KO cells relative to WT ( $13.1 \pm 0.4$  and  $16.5 \pm 0.5$  mV/ms respectively,  $t_{344} = 4.85$ ,  $P < 0.001$ ,  $n > 150$  spikes in each group). Rates of action potential fall (repolarization) were also reduced in KO cells (KO,  $-11.4 \pm 0.2$  mV/ms; WT,  $-16.7 \pm 0.4$  mV/ms;  $t_{344} = 11.66$ ,  $P < 0.001$ ,  $n > 150$  spikes in each group). In turn, action potential threshold (Fig. 3D) was significantly more positive in KO cells than in WT cells ( $-18.5 \pm 0.3$  and  $-21.4 \pm 0.2$  mV, respectively,  $t_{344} = 7.97$ ,  $P < 0.001$ ,  $n > 150$  spikes in each group). The after-hyperpolarization potential (Fig. 3B) was also more positive in KO cells ( $-40.7 \pm 0.3$  mV in KO and  $-47.3 \pm 0.3$  mV in WT,  $t_{344} = 16.67$ ,  $P < 0.001$ ,  $n > 150$  spikes in each set). These data indicate that TASK1/3 deletion reduces the intrinsic excitability of orexin cells, and disrupts their ability to generate high-frequency firing.

## Responses of orexin neurons to glucose

The percentage of orexin neurons that responded to glucose with hyperpolarization (Fig. 4A) was similar in KO mice ( $n = 10$  out of 10 cells, 100%) and WT mice (95%; Burdakov *et al.*, 2005,2006). The magnitude of glucose-induced hyperpolarization was also similar in WT and KO orexin neurons ( $25.1 \pm 3.7$  and  $21.8 \pm 2.3$  mV, respectively,  $t_{10} = 0.76$ ,  $P = 0.46$ ). As previously described for WT orexin cells (Burdakov *et al.*, 2006), the glucose-induced postsynaptic current in orexin neurons from TASK1/3 knockout mice displayed key hallmarks of a leak-like  $K^+$  current: a reversal potential corresponding to  $E_K$  and current-voltage rectification well approximated by the GHK equation (Fig. 4C). The amplitudes of glucose-induced current in WT and TASK knockouts were also not significantly different (at  $-60$  mV, WT,  $53.5 \pm 11.5$  pA; KO,  $61.9 \pm 15.0$  pA;  $n = 6$  in each group,  $t_{10} = 0.44$ ,  $P = 0.67$ ). Similar to WT orexin cells (Burdakov *et al.*, 2006), in KO cells extracellular acidification reversed both glucose-induced hyperpolarization (Fig. 4A) and activation of  $K^+$  currents (Fig. 4B). Together, these data suggest that TASK1/3 channels are not critical for glucose responses of orexin neurons.

## Locomotor responses to restricted feeding

Mice lacking orexin neurons display diminished food-anticipatory locomotor activity under restricted feeding paradigms, consistent with a role for these cells in linking metabolic state to behaviour (Yamanaka *et al.*, 2003; Mieda *et al.*, 2004). We reasoned that if TASK1 or TASK3 channels were critical metabolic sensors in orexin neurons, a similar disruption of food-anticipatory activity would be observed in TASK1/3 knockout mice. However, we found that food-anticipatory activity, measured as wheel revolutions during the 3-h period before the daily meal, was indistinguishable in TASK1/3 KO and WT mice (Fig. 4D, E, statistics are given in the figure legend). Body weights also did not differ significantly between TASK1/3 knockouts and controls at any time during the 18 days of restricted feeding, or after the subsequent 2 days of fasting (Fig. 4F, statistics are given in the figure legend).

## Responses of orexin neurons to acid

In the presence of high glucose concentration, the membrane potential of KO cells remained sensitive to extracellular pH (Fig. 4A), due to the inhibitory action of acid on  $K^+$  currents (Fig. 4B). Apart from acid-sensitive  $K^+$  channels, other acid-sensitive channels exist, for example acid-activated  $Na^+$ -permeable channels, ASICs (Krishtal, 2003; Putnam *et al.*, 2004). However, acid-induced reversal of glucose effects on the membrane potential and  $K^+$  currents persisted when ASICs were blocked with  $100 \mu M$  amiloride (Fig. 5A,  $n = 6$  cells). In the presence and absence of amiloride, acidification to pH 6 (in  $5$  mM glucose) was equally fast in depolarizing the cells back to potentials exhibited in  $1$  mM glucose ( $209 \pm 38.5$  and  $223 \pm 49.5$  s, respectively,  $P = 0.82$ ,  $t_{10} = 0.233$ ). These results suggest that ASIC channels are not essential for the depolarizing action of acid on orexin cells, although they do not rule out that acid might modulate channels/transporters other than acid-inhibited  $K^+$  channels.

To examine further the interplay between acid and pH sensing in WT orexin cells, we examined their response to glucose in alkaline solutions (pH 9), and found that the effects of glucose and high pH were additive rather than occlusive (Fig. 5B,  $n = 4$  cells), as previously suggested by a related experiment examining the response to alkaline pH in high glucose (Burdakov *et al.*, 2006). This may suggest that glucose and pH act on separate channels; alternatively, however, it may mean that glucose and pH act on the same channel(s), but that neither of these modulators can by itself attain the maximum open probability, e.g. as reported for the effects of halothane on  $K_{2P}$  channels (Sirois *et al.*, 2000). Finally, we examined the sensitivity of KO cells to changes in extracellular pH in low glucose ( $1$  mM) solutions. We found that responses of KO cells to pH were similar to those found in WT

orexin cells (Fig. 5C,  $n = 6$  cells). The firing rate of KO cells was  $0.3 \pm 0.1$  Hz at pH 7.4 and  $2.2 \pm 0.6$  Hz at pH 6.9 ( $t_5 = 4.45$ ,  $n = 6$ ,  $P = 0.007$ , paired-sample  $t$ -test), i.e. about a sevenfold increase, similar to that for WT orexin cells (~10-fold increase, Williams *et al.*, 2007). Voltage-clamp analysis of membrane current–voltage relationships (Fig. 5D) revealed, as in WT cells (Williams *et al.*, 2007), that in KO cells acid inhibited a net current with properties of a leak-like  $K^+$  current (Fig. 5E). This suggests that TASK1/3 channels are not essential for the responses of orexin neurons to changes in extracellular pH.

## Discussion

Our study presents a genetic dissection of the ion channel mechanisms regulating the firing of orexin/hypocretin neurons. The results suggest that postsynaptic TASK1/3 channels enhance membrane excitability of orexin cells and their ability to generate high-frequency firing, but that these channels are not essential for the responses of orexin cells to glucose. The lack of any differences in activity or body weight in response to food restriction supports the latter conclusion. Typical pH responses of orexin cells are also maintained in TASK1/3 KO mice.

Basic membrane biophysics predicts that removal of a leak  $K^+$  current would shift the membrane potential away from  $E_K$ , i.e. closer to the threshold for action potential (Koch, 1999; Hille, 2001). This would make the membrane more excitable, and thus leak  $K^+$  channels such as TASK are traditionally thought to limit neuronal excitability (Goldstein *et al.*, 2001). However, in the present study, TASK channel deletion made orexin cell membrane *less* able to generate action potentials. Specifically, KO cells displayed (i) reduced ability to generate high-frequency firing, (ii) reduced rate of action potential rise and (iii) a more positive action potential threshold. Although TASK channel deletion also led to a slight depolarization of the membrane potential, the latter changes were independent of this, as we corrected for this effect by collecting action potential data at the same resting potentials.

Our results are thus in support of the idea, recently proposed by Brickley *et al.* based on data from cerebellar granule cells, that TASK  $K_{2P}$  channels, in addition to their classical role of limiting excitability through membrane hyperpolarization, also have a novel effect of increasing excitability and supporting high-frequency firing, an effect traditionally associated with  $Kv3$  rather than  $K_{2P}$  channels (Lien & Jonas, 2003; Brickley *et al.*, 2007). TASK channels may enhance excitability by reducing the degree of inactivation developed by voltage-gated  $Na^+$  channels during excitatory drive, for example by increasing spike after-hyperpolarization (our data) and also by reducing the membrane time constant (see discussion in Brickley *et al.*, 2007). It should be noted that, while theoretically it is also possible that TASK deletion may affect firing indirectly by altering expression of other channel(s), this is unlikely because re-introduction of a TASK-like conductance via dynamic current-clamp restores normal firing in TASK KO cells (Brickley *et al.*, 2007).

*In vivo* data on orexin cell firing are scarce (Lee *et al.*, 2005; Mileykovskiy *et al.*, 2005), and it remains unknown under which physiological conditions orexin neurons may attain the high firing frequencies where the effects of TASK channels become evident (>70 Hz, Fig. 2C). Orexin cell firing associated with exploration and feeding occurs at a lower frequency range (~10 Hz, Mileykovskiy *et al.*, 2005), consistent with our finding of the lack of effect of TASK1/3 channel knockout on feeding-related locomotor activity. However, there are data suggesting that higher firing rates are generated by mildly stressful situations such as sudden noises (Mileykovskiy *et al.*, 2005). It is thus possible that more stressful and/or dangerous situations would make orexin cells fire at the high frequencies where TASK

channels become important; this remains to be tested by *in vivo* recordings from identified orexin neurons in behaving animals.

We have shown that glucose hyperpolarizes orexin cells in a manner not requiring conventional glucose-sensing machinery and involving activation of postsynaptic leak-like  $K^+$  currents (Burdakov *et al.*, 2006). The molecular composition of the underlying channels is difficult to address, because there are currently no selective modulators of leak  $K^+$  channels and at least 15 genes encoding these channels, theoretically giving rise to even more dimeric subunit combinations (Lesage, 2003; Talley *et al.*, 2003; Goldstein *et al.*, 2005). In our original study, we cautioned that resolution of the channel(s) molecular identity would require manipulation of multiple KCNK genes, but hypothesized that TASK1 and TASK3 subunits might be involved, based on functional data such as reversal of glucose effects by acidification (Burdakov *et al.*, 2006).

The present study directly addressed this hypothesis by genetic deletion of TASK1/3 subunits, which showed that these subunits are not essential for glucose-induced activation of leak-like  $K^+$  currents or their inhibition by acid (Fig. 4A–C). One could argue that TASK1/3 channels do mediate glucosensing in WT mice but that some compensation takes place in the KOs to maintain normal sensitivity to glucose. However, such a conclusion would require that the compensatory current has properties that are the same as the TASK1/3 current it is replacing. Although possible, this seems unlikely, and the simplest conclusion is that TASK1/3 channels are not involved. Thus, other genes encoding leak-like channels, e.g. TASK5, are likely to be more critical, and furthermore, it cannot be ruled out that proteins outside the KCNK family may also contribute. Useful information about this issue may potentially be provided by analysing the levels of expression of different  $K^+$  channel subunits in orexin neurons using quantitative PCR techniques. This is beyond the scope of the present study, and a truly definitive test of candidate channels will require reconstitution of the glucose response in heterologous systems, which will need to await better characterization of other molecular players in the glucose-sensing pathway of orexin neurons, e.g. the nature of the putative extracellular glucose receptors and intracellular signalling pathway(s) (González *et al.*, 2008).

Finally, we found that pH responses of orexin neurons were maintained in TASK1/3 KO mice (Fig. 5C). This is similar to the mouse retrotrapezoid nucleus neurons, which fully maintain their pH sensitivity in a TASK1/3 null background (Mulkey *et al.*, 2007). Thus, a pH-sensitive non-TASK  $K^+$  channel is likely to contribute to chemosensitivity of both orexin and retrotrapezoid neurons (see discussion in Mulkey *et al.*, 2007).

## Acknowledgments

This work was funded by the European Research Council (FP7 grant to D.B.), and National Institutes of Health grants NS033583 (to D.A.B.) and MH074924 (to M.M.).

## Abbreviations

<b>ACSF</b>	artificial cerebrospinal fluid
<b>GFP</b>	green fluorescent protein
<b>GHK</b>	Goldman–Hodgkin–Katz
<b>KO</b>	knockout
<b>WT</b>	wild-type

## References

- Adamantidis AR, Zhang F, Aravanis AM, Deisseroth K, de Lecea L. Neural substrates of awakening probed with optogenetic control of hypocretin neurons. *Nature*. 2007; 450:420–124. [PubMed: 17943086]
- Bean BP. The action potential in mammalian central neurons. *Nat. Rev. Neurosci.* 2007; 8:451–465. [PubMed: 17514198]
- Boutrel B, Kenny PJ, Specio SE, Martin-Fardon R, Markou A, Koob GF, de Lecea L. Role for hypocretin in mediating stress-induced reinstatement of cocaine-seeking behavior. *Proc. Natl Acad. Sci. U S A.* 2005; 102:19168–19173. [PubMed: 16357203]
- Brickley SG, Aller MI, Sandu C, Veale EL, Alder FG, Sambhi H, Mathie A, Wisden W. TASK-3 two-pore domain potassium channels enable sustained high-frequency firing in cerebellar granule neurons. *J. Neurosci.* 2007; 27:9329–9340. [PubMed: 17728447]
- Burdakov D, Gerasimenko O, Verkhatsky A. Physiological changes in glucose differentially modulate the excitability of hypothalamic melanin-concentrating hormone and orexin neurons *in situ*. *J. Neurosci.* 2005; 25:2429–2433. [PubMed: 15745970]
- Burdakov D, Jensen LT, Alexopoulos H, Williams RH, Fearon IM, O’Kelly I, Gerasimenko O, Fugger L, Verkhatsky A. Tandempore K<sup>+</sup> channels mediate inhibition of orexin neurons by glucose. *Neuron*. 2006; 50:711–722. [PubMed: 16731510]
- Eggermann E, Bayer L, Serafin M, Saint-Mieux B, Bernheim L, Machard D, Jones BE, Muhlethaler M. The wake-promoting hypocretin-orexin neurons are in an intrinsic state of membrane depolarization. *J. Neurosci.* 2003; 23:1557–1562. [PubMed: 12629156]
- Goldstein SA, Bockenbauer D, O’Kelly I, Zilberberg N. Potassium leak channels and the KCNK family of two-P-domain subunits. *Nat. Rev. Neurosci.* 2001; 2:175–184. [PubMed: 11256078]
- Goldstein SA, Bayliss DA, Kim D, Lesage F, Plant LD, Rajan S. International Union of Pharmacology. LV. Nomenclature and molecular relationships of two-P potassium channels. *Pharmacol. Rev.* 2005; 57:527–540. [PubMed: 16382106]
- González JA, Jensen LT, Fugger L, Burdakov D. Metabolism-independent sugar sensing in central orexin neurons. *Diabetes*. 2008; 57:2569–2576. [PubMed: 18591392]
- Hara J, Beuckmann CT, Nambu T, Willie JT, Chemelli RM, Sinton CM, Sugiyama F, Yagami K, Goto K, Yanagisawa M, Sakurai T. Genetic ablation of orexin neurons in mice results in narcolepsy, hypophagia, and obesity. *Neuron*. 2001; 30:345–354. [PubMed: 11394998]
- Harris GC, Wimmer M, Aston-Jones G. A role for lateral hypothalamic orexin neurons in reward seeking. *Nature*. 2005; 437:556–559. [PubMed: 16100511]
- Henze DA, Buzsáki G. Action potential threshold of hippocampal pyramidal cells *in vivo* is increased by recent spiking activity. *Neuroscience*. 2001; 105:121–130. [PubMed: 11483306]
- Hille, B. *Ion Channels of Excitable Membranes*. Sunderland, MA: Sinauer Associates, Inc; 2001.
- Koch, C. *Biophysics of Computation*. New York: Oxford University Press; 1999.
- Krishtal O. The ASICs: signaling molecules? Modulators? *Trends Neurosci.* 2003; 26:477–483. [PubMed: 12948658]
- de Lecea L, Kilduff TS, Peyron C, Gao X, Foye PE, Danielson PE, Fukuhara C, Battenberg EL, Gautvik VT, Bartlett FS II, Frankel WN, van den Pol AN, Bloom FE, Gautvik KM, Sutcliffe JG. The hypocretins: hypothalamus-specific peptides with neuroexcitatory activity. *Proc. Natl Acad. Sci. U S A.* 1998; 95:322–327. [PubMed: 9419374]
- Lee MG, Hassani OK, Jones BE. Discharge of identified orexin/hypocretin neurons across the sleep-waking cycle. *J. Neurosci.* 2005; 25:6716–6720. [PubMed: 16014733]
- Lesage F. Pharmacology of neuronal background potassium channels. *Neuropharmacology*. 2003; 44:1–7. [PubMed: 12559116]
- Lesage F, Lazdunski M. Molecular and functional properties of two-pore-domain potassium channels. *Am. J. Physiol. Renal. Physiol.* 2000; 279:F793–F801. [PubMed: 11053038]
- Li Y, van den Pol AN. Mu-opioid receptor-mediated depression of the hypothalamic hypocretin/orexin arousal system. *J. Neurosci.* 2008; 28:2814–2819. [PubMed: 18337411]



- Li Y, Gao XB, Sakurai T, van den Pol AN. Hypocretin/Orexin excites hypocretin neurons via a local glutamate neuron-A potential mechanism for orchestrating the hypothalamic arousal system. *Neuron*. 2002; 36:1169–1181. [PubMed: 12495630]
- Lien CC, Jonas P. Kv3 potassium conductance is necessary and kinetically optimized for high-frequency action potential generation in hippocampal interneurons. *J. Neurosci*. 2003; 23:2058–2068. [PubMed: 12657664]
- Mieda M, Williams SC, Sinton CM, Richardson JA, Sakurai T, Yanagisawa M. Orexin neurons function in an efferent pathway of a food-entrainable circadian oscillator in eliciting food-anticipatory activity and wakefulness. *J. Neurosci*. 2004; 24:10493–10501. [PubMed: 15548664]
- Mileykovskiy BY, Kiyashchenko LI, Siegel JM. Behavioral correlates of activity in identified hypocretin/orexin neurons. *Neuron*. 2005; 46:787–798. [PubMed: 15924864]
- Mulkey DK, Talley EM, Stornetta RL, Siegel AR, West GH, Chen X, Sen N, Mistry AM, Guyenet PG, Bayliss DA. TASK channels determine pH sensitivity in select respiratory neurons but do not contribute to central respiratory chemosensitivity. *J. Neurosci*. 2007; 27:14049–14058. [PubMed: 18094244]
- Patel AJ, Honore AE. Properties and modulation of mammalian 2P domain K<sup>+</sup> channels. *Trends Neurosci*. 2001; 24:339–346. [PubMed: 11356506]
- Peyron C, Tighe DK, van den Pol AN, de Lecea L, Heller HC, Sutcliffe JG, Kilduff TS. Neurons containing hypocretin (orexin) project to multiple neuronal systems. *J. Neurosci*. 1998; 18:9996–10015. [PubMed: 9822755]
- Putnam RW, Filosa JA, Ritucci NA. Cellular mechanisms involved in CO<sub>2</sub> and acid signaling in chemosensitive neurons. *Am. J. Physiol. Cell Physiol*. 2004; 287:C1493–C1526. [PubMed: 15525685]
- Sakurai T. The neural circuit of orexin (hypocretin): maintaining sleep and wakefulness. *Nat. Rev. Neurosci*. 2007; 8:171–181. [PubMed: 17299454]
- Sakurai T, Amemiya A, Ishii M, Matsuzaki I, Chemelli RM, Tanaka H, Williams SC, Richardson JA, Kozlowski GP, Wilson S, Arch JR, Buckingham RE, Haynes AC, Carr SA, Annan RS, McNulty DE, Liu WS, Terrett JA, Elshourbagy NA, Bergsma DJ, Yanagisawa M. Orexins and orexin receptors: a family of hypothalamic neuropeptides and G protein-coupled receptors that regulate feeding behavior. *Cell*. 1998; 92:573–585. [PubMed: 9491897]
- Sirois JE, Lei Q, Talley EM, Lynch C III, Bayliss DA. The TASK-1 two-pore domain K<sup>+</sup> channel is a molecular substrate for neuronal effects of inhalation anesthetics. *J. Neurosci*. 2000; 20:6347–6354. [PubMed: 10964940]
- Talley EM, Sirois JE, Lei Q, Bayliss DA. Two-pore-Domain (KCNK) potassium channels: dynamic roles in neuronal function. *Neuroscientist*. 2003; 9:46–56. [PubMed: 12580339]
- Tsunematsu T, Fu LY, Yamanaka A, Ichiki K, Tanoue A, Sakurai T, van den Pol AN. Vasopressin increases locomotion through a V1a receptor in orexin/hypocretin neurons: implications for water homeostasis. *J. Neurosci*. 2008; 28:228–238. [PubMed: 18171940]
- Williams RH, Jensen LT, Verkhatsky A, Fugger L, Burdakov D. Control of hypothalamic orexin neurons by acid and CO<sub>2</sub>. *Proc. Natl Acad. Sci. U S A*. 2007; 104:10685–10690. [PubMed: 17563364]
- Winsky-Sommerer R, Yamanaka A, Diano S, Borok E, Roberts AJ, Sakurai T, Kilduff TS, Horvath TL, de Lecea TL. Interaction between the corticotropin-releasing factor system and hypocretins (orexins): a novel circuit mediating stress response. *J. Neurosci*. 2004; 24:11439–11448. [PubMed: 15601950]
- Yamanaka A, Beuckmann CT, Willie JT, Hara J, Tsujino N, Mieda M, Tominaga M, Yagami K, Sugiyama F, Goto K, Yanagisawa M, Sakurai T. Hypothalamic orexin neurons regulate arousal according to energy balance in mice. *Neuron*. 2003; 38:701–713. [PubMed: 12797956]

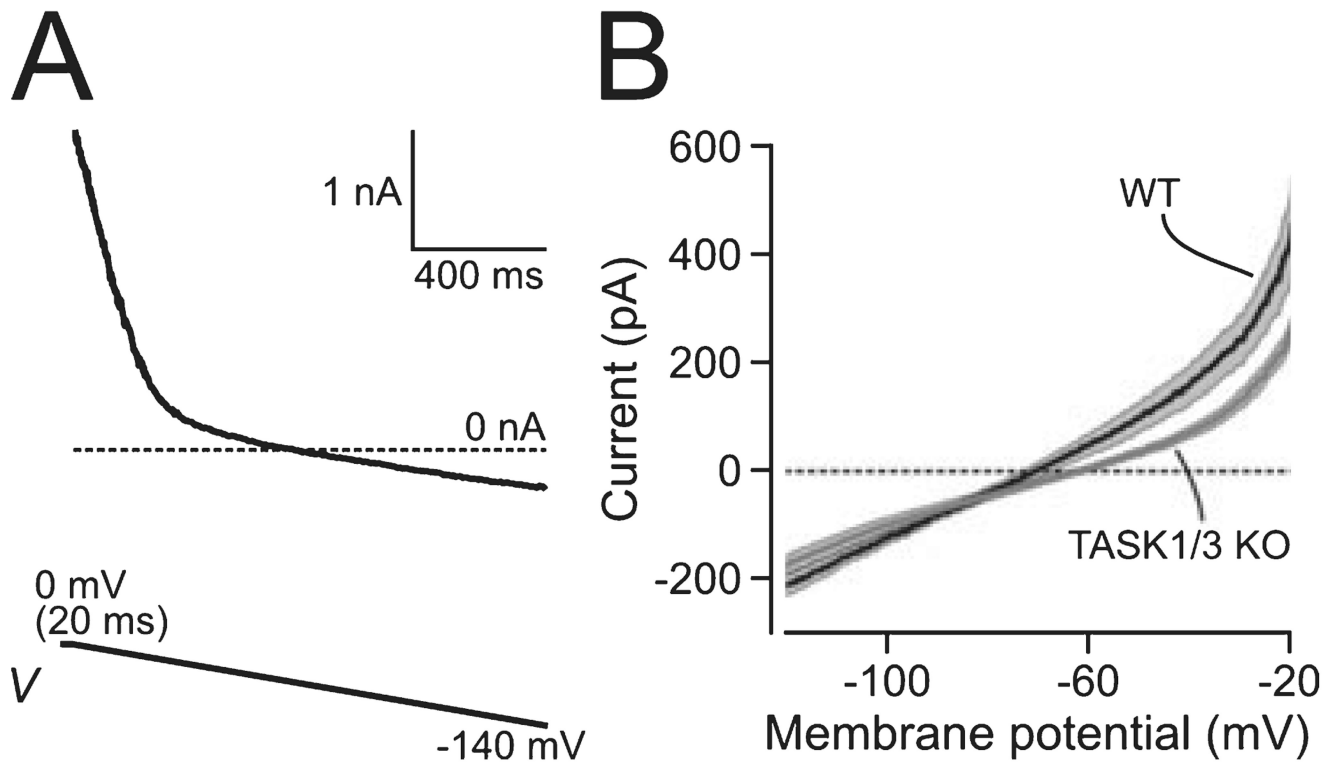


**FIG. 1. Effect of TASK1/3 knockout on whole-cell current of orexin cells**  
 (A) Voltage-clamp ramp protocol used to obtain whole-cell  $I-V$  relationship. The current trace is an example of raw data from one cell, and the protocol is shown schematically below the trace. (B)  $I-V$  relationships of WT ( $n = 6$ ) and KO cells ( $n = 16$ ). Values are means  $\pm$  SEM; the SEM values are shown shaded around the bold lines showing means.

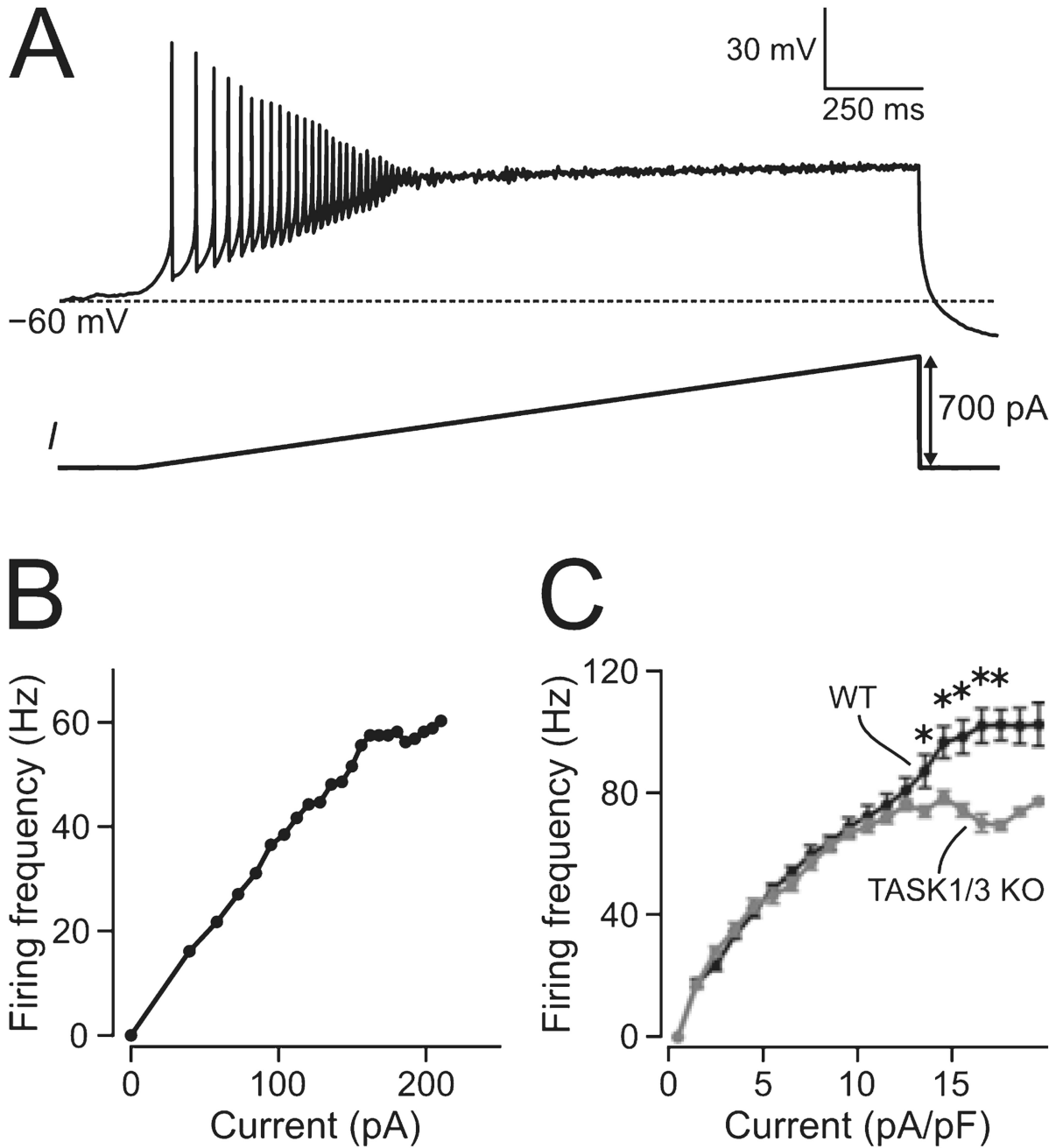


**FIG. 2. Effect of TASK1/3 knockout on excitability of orexin cells**

(A) Illustration of the current-clamp protocol used to measure firing-current relationships; a typical raw-data trace from a WT cell is shown above the protocol schematic. (B) An example of a firing-current plot, calculated from inter-spike intervals of the recording shown in A. (C) Mean firing-current relationships in WT and KO cells (ten cells in each group). \* $P < 0.01$ .

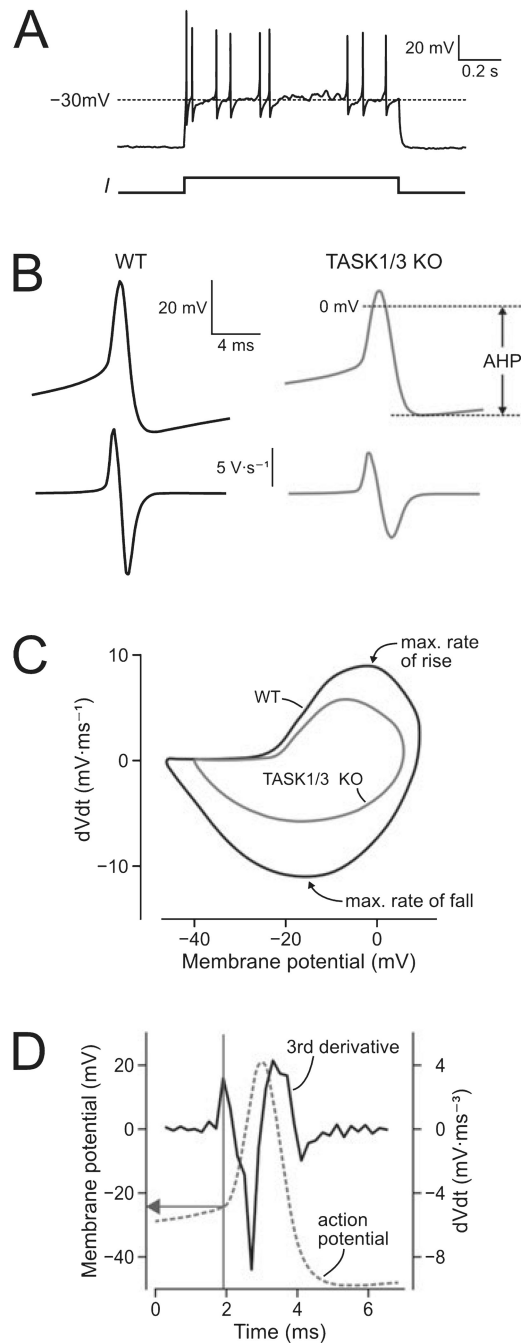


**FIG. 3. Effect of TASK1/3 knockout on individual action potentials of orexin cells**

(A) An example of raw data used for analysis; spikes initiated from the same resting potential ( $-30$  mV) were analysed. (B) Top traces: action potentials in WT and KO cells (mean values of 193 and 153 spikes, respectively, obtained from nine WT and ten KO neurons). Bottom traces: first derivative values of corresponding top traces, used to produce the plots in C. (C) Phase-plane plots of action potential shape in WT and KO cells (mean values of 193 and 153 spikes, respectively). (D) Graphical illustration of the 3rd derivative method used to determine the action potential threshold.

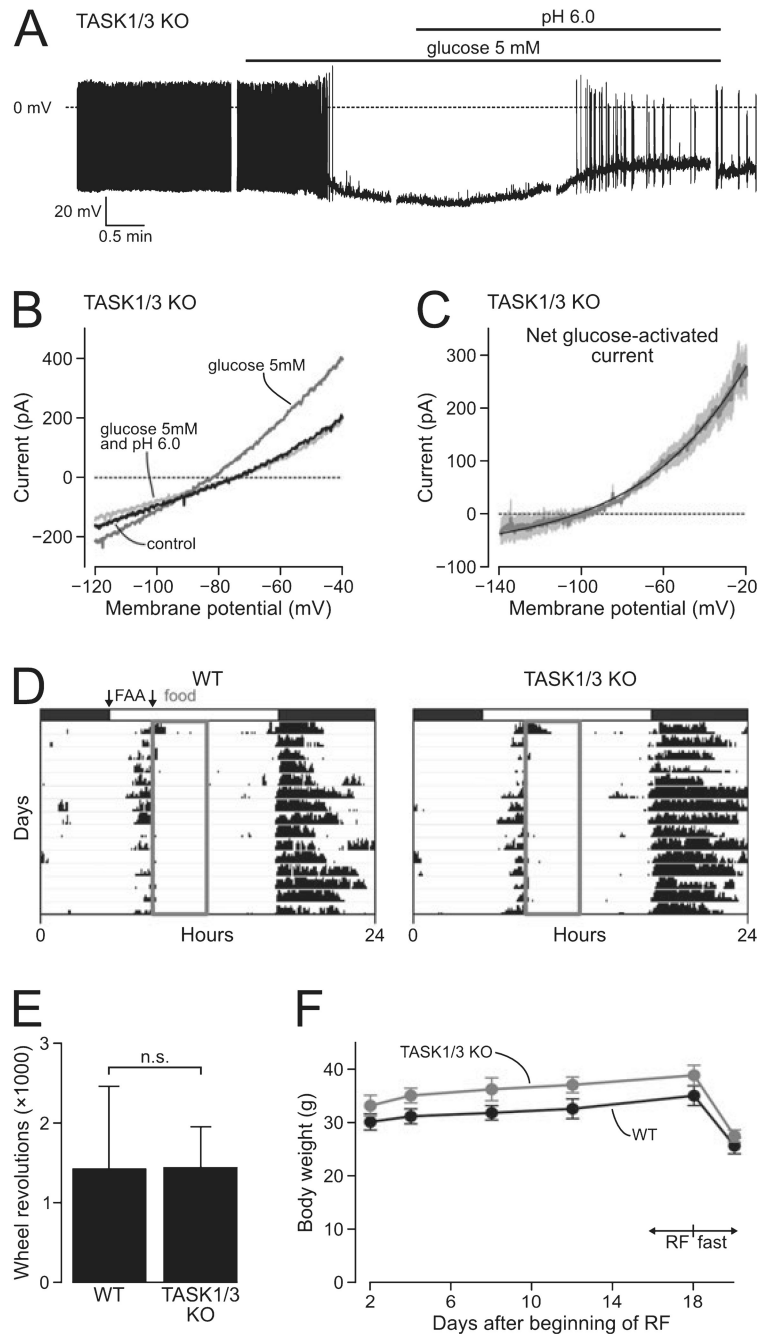


**FIG. 4. Effect of TASK1/3 knockout on glucose-sensing and food-anticipatory activity**  
 (A) A typical membrane potential response of a KO cell to glucose and subsequent extracellular acidification. Breaks in the trace are due to pauses in the recording during which voltage-clamp measurements were taken. (B) A typical membrane current response of a KO cell to glucose and subsequent extracellular acidification (measured using the ramp protocol as in Fig. 1). (C) Current–voltage relationship of the net glucose-activated current in KO cells. Mean values are shown in grey ( $n = 4$  cells), SEMs are in lighter shading. The black line shows a fit of the Goldman–Hodgkin–Katz equation to the data. (D) Typical records of median wheel-running activity from four WT and four KO mice during days when food was only available for 4 h per day (grey box). Animals were maintained on a

12/12-h light–dark cycle (indicated by white and black bars). Arrows indicate the 3-h period where food-anticipatory activity (FAA) was measured. (E) Mean total FAA (18 days) in WT and KO mice. n.s. = not significant ( $t_6 = 0.01$ ,  $P = 0.99$ ). (F) Mean body weights for WT and KO mice during the restricted feeding (RF) and subsequent fasting. No significant differences were found ( $P > 0.05$ , ANOVA, Tukey's *posthoc* comparison).

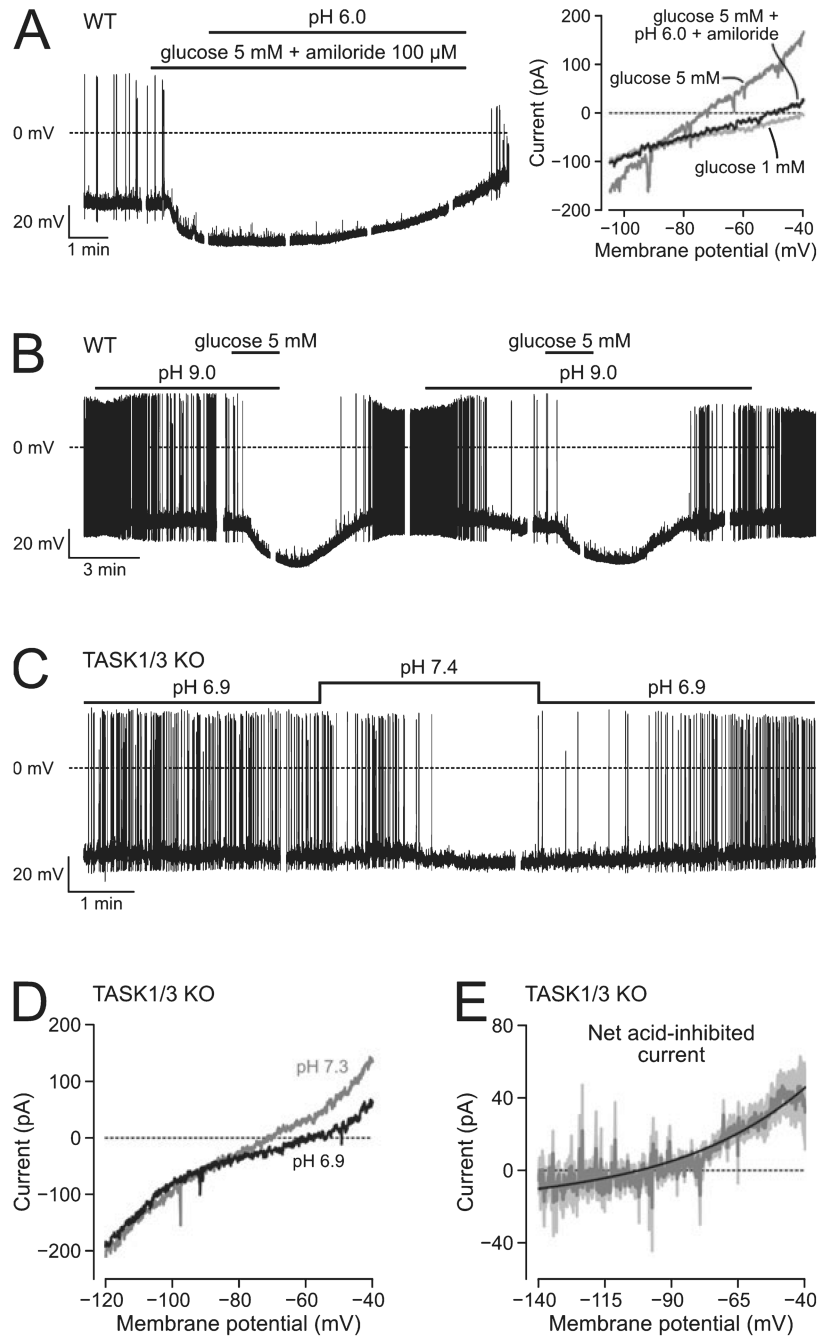


### FIG. 5. Effect of pH on WT and TASK1/3 KO orexin cells

(A) Amiloride does not prevent the reversal of glucose response by acid pH. Left trace: example of acid-induced reversal of membrane potential response. Right trace: example of acid-induced block of glucose-stimulated  $K^+$  current (representative examples of  $n=6$  cells). (B) Alkaline pH does not occlude the response to glucose ( $n=4$  cells). (C) The firing of KO cells remains sensitive to extracellular pH ( $n=6$  cells). (D) Example of the effect of pH on the current–voltage relationship of a KO cell. (E) Net current inhibited by acid in KO cells, obtained from data such as shown in D; mean values ( $n=4$  cells) are shown in dark grey and SEM values in lighter shading; the black line is a fit of the Goldman–Hodgkin–Katz equation to the data.